LVI SBPO SIMPÓSIO BRASILEIRO DE PESQUISA OPERACIONAL
DE 04 ATÉ 07 NOVEMBRO 2024
FORTALEZA | CEARÁ

# Automated Picking of Time-Velocity Pairs Using a Hybrid Grey Wolf Optimizer

**Arthur A. C. R. Silva**
*Graduate Program on Systems and Computing, UFRN, Natal, Brazil*
arthur.romao@ufrn.br

**Bruno M. Carvalho**
*Department of Informatics and Applied Mathematics, UFRN, Natal, Brazil*
bruno@dimap.ufrn.br

## ABSTRACT

Reflection seismic is crucial for geophysical exploration, analyzing Earth's subsurface layers through reflected waves. The precision of Normal MoveOut (NMO) correction greatly influences effectiveness, requiring careful selection of time-velocity pairs. Manual selection is challenging due to diverse, extensive field data. Our study automates this process using the Semblance coherence panel, identifying coherent patterns to optimize pair picking. This approach has yielded promising results. The *Hybrid Grey Wolf Optimizer* (*HGWO*), incorporating genetic operators and *Simulated Annealing* (*SA*) algorithms, was employed for automated pair picking. Wilcoxon tests confirmed their equivalence and acceptable solutions, showing correct minimization of the objective function and algorithmic convergence to accurate pairs. Automation simplifies the process, enhancing the quality and accuracy of geological interpretations, refining analysis of reflection seismic data. Integrating Semblance into automated picking represents a significant advancement, streamlining procedures and improving reliability. This is vital for accurate decision-making in exploratory studies and geological mapping.

**KEYWORDS. Reflection Seismic, Picking Time-Velocity Pairs, Bio-inspired Optimization.**

## 1. Introduction

The analysis of velocity plays a crucial role in seismic data processing, enabling the estimation of geological characteristics of subsurface layers based on the reflection times of seismic waves as they traverse and are detected by geophones. However, the manual selection of time-velocity pairs, representing the maximum energy values in the semblance spectrum, is a time-consuming and demanding process, especially when dealing with extensive seismic datasets [Yilmaz, 2001].

To streamline and expedite this process, automated techniques have been developed. Optimization algorithms have excelled in this area, seeking the most efficient and accurate time-velocity pairs [Huang et al., 2013; Velis, 2021; Fortini et al., 2013]. In this study, we employed both the *Hybrid Grey Wolf Optimizer* (*HGWO*) with genetic crossover and mutation operators, along with the inclusion of tournament and elitism steps, and *Simulated Annealing* (*SA*). The GWO, inspired by the behavior of a pack of grey wolves, has demonstrated effectiveness in solving nonlinear optimization problems, capable of finding optimal or near-optimal solutions [Song et al., 2015; Vashisth et al., 2022; Li et al., 2018].

By applying the *Hybrid Grey Wolf Optimizer* to the automatic selection of time-velocity pairs, we significantly reduce the time and effort involved in this task. The algorithm seeks to identify the best time-velocity combinations in the semblance spectrum, thereby improving the

**DOI:** 10.59254/sbpo-2024-193821
https://proceedings.science/p/193821?lang=pt-br

accuracy and effectiveness of velocity analysis. Additionally, the automatic selection provided by GWO efficiently handles large seismic datasets, enabling quicker and more precise analysis.

*Simulated Annealing*, another powerful optimization algorithm, will also be employed in this study [Kirkpatrick et al., 1983]. We will compare the performance of *Simulated Annealing* and the *Grey Wolf Optimizer* under various criteria using the Wilcoxon hypothesis test. The use of these optimization algorithms for the automatic selection of time-velocity pairs in semblance expedites the velocity analysis process and ensures more reliable results. This contributes to enhancing the quality of processed seismic data and facilitates interpretation, aiding in areas such as oil and gas exploration, geotechnical studies, and geological mapping [Payton, 1977; Alsadi et al., 2017; Mondol, 2010; Milkereit et al., 1996]. Moreover, automating this process frees up time for experts to focus on more complex tasks and the analysis of obtained results.

## 2. Reflection Seismic

Reflection seismology is a widely utilized technique in the oil and gas exploration industry for mapping subsurface characteristics. This method involves a controlled generation of seismic waves into the subsurface and recording the waves reflected by geological interfaces, yielding information about the subsurface's structure and properties, including the location of hydrocarbon reservoirs [Telford et al., 1990; Sheriff and Geldart, 1995]. A fundamental equation in reflection seismology is the transit time equation, given by:

$$t^2 = t_0^2 + \frac{x^2}{v^2}. \tag{1}$$

This equation relates the transit time, denoted by $t$, with the distance traveled by the seismic wave, represented by $x$, and the wave propagation velocity in the medium, represented by $v$. The term $t_0$ signifies the initial launch time of the wave. The transit time equation describes the connection between the transit time and the distance covered by a seismic wave in a homogeneous medium. It is derived from the principle that the wave travels a straight path between the launch point and the reflection point. This equation is fundamental in reflection seismology as it facilitates the estimation of the depth of geological interfaces and provides information about the subsurface structure [Kearey et al., 2002].

In terrestrial applications, seismic waves originate from sources such as hydraulic hammers or explosives, serving as emitters. These waves traverse subsurface layers and return to geophones, sensors designed to capture the reflected waves. In the oceanic context, an example of equipment employed for generating seismic waves is the Air Gun [Larner et al., 1982]. This device comprises a compressed air cylinder connected to an expansion chamber. When activated, the compressed air is rapidly released into the water, creating a controlled explosion that generates an acoustic pressure wave. This wave propagates through the water, reaching the subsurface layers of the ocean and the rocks beneath the seafloor, subsequently reflecting back to the surface. Hydrophones, submerged acoustic sensors, are used to detect and record these reflected waves, enabling the analysis and interpretation of the obtained seismic data.

The described process produces a seismogram, as illustrated on the left side of Fig. 1, which serves as one of the experimental models in the current study. The seismogram is characterized by a horizontal axis representing the distance between the acoustic wave emitter and the receivers, while the vertical axis corresponds to time. Each hyperbola depicted in the seismogram corresponds to the reflection interface between two geological layers. Additionally, multiples are observed, representing refractions that occur in the seismic waves within each of these layers.

**DOI:** 10.59254/sbpo-2024-193821
https://proceedings.science/p/193821?lang=pt-br

## 3. Semblance

The semblance measure is a vital metric for evaluating the similarity between observed and synthetic seismic records. It is calculated through an analysis of coherence characteristics in recorded waveforms. A higher value of this metric indicates a closer match between records, instilling confidence that the selected time-velocity pairs accurately represent subsurface reflections [Kearey et al., 2002].

The panel, depicted at the center of Fig. 1, visually represents the characteristics of seismic waves reflected in subsurface layers. Constructed by comparing signals recorded by geophones at various positions, it plays a crucial role in identifying seismic events and determining the geological structure of subsurface layers. This measure is computed based on temporal correlations between received signals, indicating the degree of similarity between waveform shapes. Equation 2 represents the calculation of *Semblance*:

$$S = \frac{1}{M} \frac{\sum_{k=-K}^{K} \sum_{j=1}^{M} f_{j,k}(j)}{\sum_{k=-K}^{K} \sum_{j=1}^{M} f_{j,k}^{2}(j)}, \tag{2}$$

where $K$ is half the length of the vertical analysis window, $f_{j,k}(j)$ represents the amplitude value at the $j$-th trace at transit time $t(j)$, and $M$ is the number of traces in the CMP (Common Midpoint) gather Yilmaz [2001]. CMP gathering enhances seismic signal quality and reduces background noise for a more accurate subsurface image.

The *Semblance* panel aids in selecting time-velocity pairs, representing optimal combinations yielding high *Semblance* values in the spectrum. It enables the identification of combinations with the highest *Semblance* values, providing more accurate estimates for seismic wave velocities.

This detailed analysis of the *Semblance* panel is crucial for accurately interpreting seismic data, informing decisions in areas such as oil and gas exploration, geotechnical studies, and geological mapping. It provides valuable insights into the subsurface, facilitating an understanding of geological structure and aiding in the identification of natural resources and geological risks.

## 4. Normal MoveOut (NMO) Correction

The Normal MoveOut (NMO) correction, also known as stacking correction, plays a crucial role in seismic data processing. Its purpose is to correct temporal distortions in seismic waveforms caused by varying velocities in subsurface layers. As seismic waves propagate through geological layers, variable delays occur due to different propagation velocities in each layer. These delays result in asymmetric arrivals of waves at receivers, affecting recorded waveforms [Kearey et al., 2002].

To perform NMO correction, it is necessary to calculate the appropriate time shift to correctly align the arrivals of seismic waves with the expected ideal transit times for each reflection. This calculation takes into account estimates of subsurface layer velocities.

By determining the necessary time shift in each time interval, NMO correction can be applied to seismic waveforms. This shifting process compensates for delays caused by different velocities, resulting in correctly aligned waveforms.

Fig. 1 presents, in the center, a *Semblance* panel containing selected time-velocity pairs that best characterize the observed seismic event. These points demonstrate higher coherence based on subsurface geological features, providing a more accurate explanation of the reflection behavior at interfaces. On the left, there is the seismogram generated from data obtained from seismic traces. Finally, on the right, are the seismogram data after NMO correction.

In summary, NMO correction is a fundamental technique for improving the quality of seismic data, minimizing distortions, and enabling a more precise interpretation of reflections from

**DOI:** 10.59254/sbpo-2024-193821
https://proceedings.science/p/193821?lang=pt-br

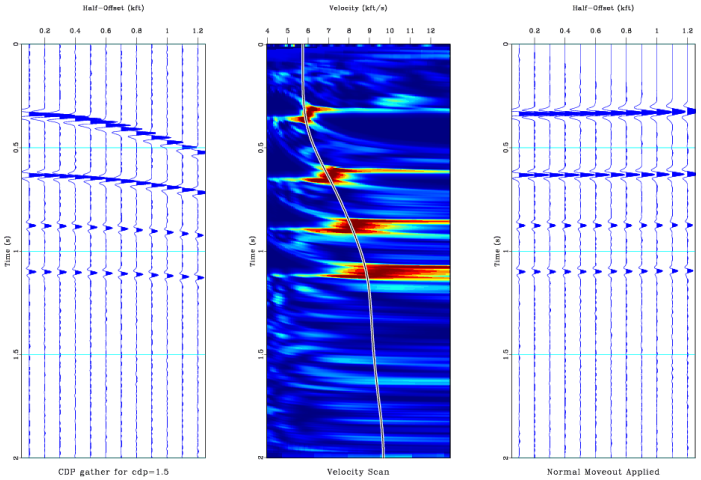



Figure 1: Example of NMO correction applied to seismic data. Adapted from Madagascar Development Blog, Open Source Software, `https://reproducibility.org/blog/2013/04/08/program-of-the-month-sfnmo/`.

subsurface layers. Additionally, it is a crucial step in the stacking process, where corrected waveforms are combined to form a more coherent and higher-resolution seismic image.

## 5. Velocity Analysis

In seismic data processing, velocity analysis plays a crucial role. The goal of this stage is to determine the velocity of seismic waves in the subsurface, which is essential for correcting the moveout effect in recorded reflections. Moveout occurs due to the varied distances traveled by seismic waves from the subsurface to the receivers, depending on the depth of reflecting interfaces [Kearey et al., 2002].

Picking time-velocity pairs is a critical step in velocity analysis. In this process, appropriate pairs of reflection arrival times and associated velocities are selected to best represent the seismic characteristics of the subsurface. These pairs are chosen to maximize the semblance, a measure of similarity, between observed seismic records and synthetic records generated with different time-velocity pairs [Yilmaz, 2001].

In this study, based on the approach by Velis [2021] using the *Simulated Annealing* method, we applied similar principles but used the *Grey Wolf Optimizer* algorithm. The objective was to create the cost function $J$ to be minimized, aiming to find time-velocity pairs providing the most satisfactory NMO correction.

The cost function $J$ is defined by Equation 3:

$$J = 1 - \frac{1}{N}\sum_{i=1}^{N} \sigma_i(t_0^i, V_{NMO}^i), \tag{3}$$

where $\sigma_i$ represents the semblance calculated along the $i$-th hyperbolic event defined by the corresponding pair $(t_0^i, V_{NMO}^i)$. In this work, we used the semblance commonly employed in conventional velocity analysis, given by Equation 4:

$$\sigma_i(t_0^i, V_{NMO}^i) = \frac{\sum_{k=-K}^{K}\left[\sum_{j=1}^{M} s_j(t_i + k\Delta t)\right]}{M\sum_{k=-K}^{K}\sum_{j=1}^{M}\left[s_j(t_i + k\Delta t)\right]}, \tag{4}$$

**DOI:** 10.59254/sbpo-2024-193821
https://proceedings.science/p/193821?lang=pt-br

where $s_j$ represents the $j$-th trace ($j = 1, ..., M$), $K$ is half the length of the vertical analysis window used to calculate the semblance mean, and $t_i$ is given by:

$$t_i = \sqrt{t_0^i + \frac{x_j^2}{V_{NMO}^i}}. \tag{5}$$

Additionally, constraints for the parameters were incorporated to obtain ordered solutions representing events in a linear format. The constraints are defined by Equations 6 and 7:

$$t_0^{i-1} + \delta t_0 \leq t_0^i \leq t_0^{i+1} - \delta t_0, \tag{6}$$

$$V_{NMO}^{i-1} + \delta V_{NMO} \leq V_{NMO}^i \leq V_{NMO}^{i+1} - \delta V_{NMO}. \tag{7}$$

These constraints are essential to prevent the algorithm from converging to a set of time-velocity pairs in a single region that maximizes the semblance energy. Thus, we adjust the solution to a line representing different events during the seismic wave emission, reflection, and reception process.

## 6. Global Optimization

Global optimization methods are algorithms used to find the optimal solution to an optimization problem by comprehensively exploring the entire search space. In contrast to local optimization methods that aim to find the local minimum of a function, global optimization methods seek the global minimum, considering all possible solutions [Horst et al., 2000; Horst and Pardalos, 2013].

One of the main advantages of global optimization methods is their ability to explore a broader search space, enabling the discovery of solutions that might otherwise be overlooked by local optimization algorithms. This is particularly useful in complex problems where the objective function may have multiple local minima, and the goal is to find the best global solution [Horst et al., 2000; Horst and Pardalos, 2013; Törn and Žilinskas, 1989].

Another advantage of global optimization methods is their capability to handle nonlinear, nondifferentiable, or multi-constrained functions. These methods are more flexible and can be applied to a wide range of problems, including engineering, economics, science, and more [Sen and Stoffa, 2013; Hein, 1994].

Furthermore, global optimization methods are generally robust and provide theoretical guarantees of convergence to the optimal solution. This means that if the algorithm is executed correctly, it is possible to obtain a solution close to the global minimum with high probability [Granville et al., 1994].

### 6.1. Simulated Annealing

*Simulated Annealing*, a highly effective approach for tackling optimization problems in intricate and non-convex search spaces, carefully balances exploration and exploitation, akin to the annealing process in metallurgy. Drawing inspiration from metallurgical annealing, this method is a probabilistic optimization algorithm that emulates the gradual cooling of materials to attain a low-energy state. Through iterative exploration of the solution space, it probabilistically embraces inferior solutions to navigate away from local minima.

The algorithm incorporates a temperature parameter, controlling the likelihood of accepting suboptimal solutions, which gradually diminishes over iterations. This temperature-driven strategy facilitates a harmonious interplay between exploration and exploitation throughout the optimization process [Kirkpatrick et al., 1983].

The *Simulated Annealing* algorithm begins by randomly initializing a solution and setting an initial temperature. It iteratively generates neighboring solutions, evaluates their cost function,

**DOI:** 10.59254/sbpo-2024-193821
https://proceedings.science/p/193821?lang=pt-br

Initialize solution $X$ randomly;
Initialize temperature $T$;
Set cooling rate $\alpha$;
Initialize iteration counter $iter$;
**while** *Stopping criterion not met* **do**
  Generate a neighboring solution $X_{\text{new}}$ by perturbing $X$;
  Evaluate the cost function for $X$ and $X_{\text{new}}$;
  **if** $rand(0,1) < e^{-\frac{f(X_{new})-f(X)}{T}}$ **then**
    Accept $X_{\text{new}}$ as the current solution;
  **end**
  Update temperature: $T \leftarrow T \times \alpha$;
  Increment iteration counter: $iter \leftarrow iter + 1$;
**end**
Return the best solution found;

**Algorithm 1:** Simulated Annealing

and probabilistically accepts worse solutions based on the temperature parameter. The temperature gradually decreases, controlling the acceptance probability and facilitating the algorithm's transition from exploration to exploitation. The process continues until a stopping criterion is met. The version used in this context is based on Vandekerckhove [2008].

The pseudocode for *Simulated Annealing* is depicted in Algorithm 1. Key components include the initialization of the solution and temperature, the generation of neighboring solutions, the evaluation of the cost function, and the acceptance of solutions based on a probability condition. The temperature is updated in each iteration, and the algorithm concludes by returning the best solution found during the exploration.

### 6.2. Grey Wolf Optimizer

The *Grey Wolf Optimizer* (*GWO*) is an optimization algorithm inspired by the hunting behavior of a pack of grey wolves in their natural habitat. Introduced by [Mirjalili et al., 2014; Saremi et al., 2015], this algorithm utilizes a mathematical modeling of decision and control parameters based on the biological principles of wolf pack hierarchy. The GWO involves the social categorization of wolves within the pack, hunting a prey (objective), encircling the prey for cornering, and attacking the prey.

Utilizing GWO as a global optimization method offers several advantages. Firstly, its pack behavior-based approach allows for a broad exploration of the search space, increasing the likelihood of finding the global minimum. Additionally, GWO is relatively straightforward to implement and tune, making it a viable choice for a diverse array of optimization problems. The algorithm begins by randomly generating a pack of wolves, each characterized by a set of decision parameters. These parameters are represented by vectors $a$, $A$, and $C$, which play a crucial role in determining the wolves' movements and interactions during the optimization process. The fitness of each wolf is evaluated based on its ability to approximate the optimal solution to the given problem.

During each iteration, every wolf in the pack updates its position in the search space. This movement is influenced by the hierarchical structure within the pack, where three dominant individuals, denoted as $X_\alpha$, $X_\beta$, and $X_\delta$, guide the direction of the entire pack. The updating process involves adjusting the position of each search agent according to its current location and the influence of the three leaders.

Additionally, the algorithm dynamically adapts the coefficients $a$, $A$, and $C$ to enhance

**DOI:** 10.59254/sbpo-2024-193821
https://proceedings.science/p/193821?lang=pt-br

Randomly generate the wolf pack;
Create vectors of coefficients $a$, $A$, and $C$;
Evaluate the fitness of each search agent in the pack:
$X_\alpha$ = Best agent in the pack;
$X_\beta$ = Second-best agent in the pack;
$X_\delta$ = Third-best agent in the pack;
**while** *Stopping criterion not met* **do**
  **foreach** *wolf* $\mathbf{s}_i$ *in the pack* **do**
    Update the position of each search agent;
  **end**
  Update coefficients $a$, $A$, and $C$;
  Evaluate the fitness of each search agent in the pack;
  Update agents $X\alpha$, $X_\beta$, and $X_\delta$;
**end**
Return $X_\alpha$;

**Algorithm 2:** Grey Wolf Optimizer

the exploration and exploitation capabilities of the wolf pack. These coefficients control the step sizes and movement magnitudes of the wolves, allowing for a balanced exploration of the solution space while ensuring a focused search around promising regions.

The GWO continues iterating until a predefined stopping criterion is met. Throughout the iterations, the algorithm refines the positions of the wolves, updates the dominance hierarchy, and adjusts the control parameters. The final output is the best solution found, represented by the position of the alpha wolf ($X_\alpha$), which corresponds to the global optimum of the optimization problem.

In summary, the *Grey Wolf Optimizer* leverages the collaborative nature of wolf packs, incorporating a hierarchical structure and dynamic parameter adaptation to efficiently explore and converge towards optimal solutions in diverse optimization scenarios.

### 6.2.1. Integration with Genetic Operators

In this research, we incorporate genetic operators into the *Grey Wolf Optimizer* (*GWO*) for optimization purposes, introducing mutation, crossover, tournament, and elitism [Holland, 1992; Goldberg and Richardson, 1987]. This hybrid approach combines the grey wolf heuristic search with genetic strategies, resulting in an enhanced exploration and exploitation of the solution space.

The process begins by generating and evaluating initial positions for the grey wolves using the objective function. Dynamic updates take place during iterations, guided by the alpha, beta, and delta concepts, where their influence is weighted by the decreasing parameter $a$. To explore new solutions, a crossover process randomly selects parents, applies crossover to produce offspring, and introduces additional variation through mutation. Tournament selection is employed to maintain population diversity, ensuring that promising solutions advance to the next generation.

Elitism is incorporated to preserve the best solutions across generations, ranking and retaining top-performing individuals. Mechanisms are implemented to keep wolf positions within defined search space limits, ensuring adherence to the solution space. After each iteration, the best individual, represented by the alpha wolf, is recorded along with its score for analysis and monitoring of the optimization process.

## 7. Methodology

In this study, we utilized the Matlab programming language to implement seismic processing and optimization algorithms [MathWorks, 2018]. Seismic processing was conducted using

**DOI:** 10.59254/sbpo-2024-193821
https://proceedings.science/p/193821?lang=pt-br

the SeismicLab package, accessible at `http://seismic-lab.physics.ualberta.ca/`. SeismicLab, tailored for seismic data processing in the Matlab environment, serves both research and educational purposes. The package includes scripts for reading and writing data in the SU format (used by Seismic Unix), with notable capabilities for straightforward SEGY header evaluation in Matlab. *Simulated Annealing* and the *Grey Wolf Optimizer*, incorporating genetic crossover and mutation operators, as well as tournament selection and elitism, were employed in our study.

For the *Hybrid Grey Wolf Optimizer*, crucial parameters include the maximum number of iterations ($\tau$), population size ($Q_{\text{size}}$), lower ($\delta_{\text{lb}}$), and upper ($\delta_{\text{up}}$) bounds, crossover rate ($P_c$), mutation rate ($P_m$), mutation magnitude ($\sigma_m$), and tournament size ($\rho_t$). The specific values assigned to these parameters, determined through empirical experimentation, are respectively 100, 100, 0.75, 0.01, and 0.1. This study employed Arithmetic Crossover or Blending Crossover for genetic algorithm crossover, combining genes from two parents to generate offspring, thereby promoting genetic diversity in the population [Michalewicz, 1992].

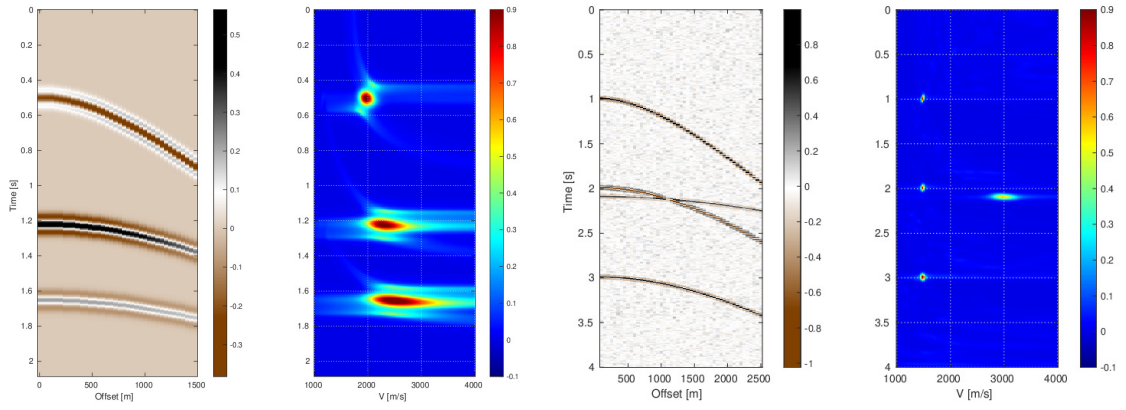
For *Simulated Annealing*, based on Vandekerckhove [2008], the parameters included the number of iterations ($\tau$), identical to that of *HGWO*, and the initial solution ($X_0$) generated at each iteration as follows: $\vec{X_0} \leftarrow \text{lb} + \text{random}(\Psi) \cdot (\text{ub} - \text{lb})$. Here, $lb$ and $ub$ are the lower and upper bounds, respectively, described in the sections of each dataset, and $\Psi$ is the size of the bounds vector.

For both algorithms, 10 rounds were conducted, and the solutions were averaged.

### 7.1. First Synthetic Data

The analysis commenced with the synthetic data `syn_cmp.su`, provided by the data package, representing a seismic event with 38 traces. The default Semblance parameters for these synthetic events included a velocity range from 1,000 to 4,000 km/s, a window size of 15, and a maximum stretch of 400.

Both algorithms were employed to search for time-velocity pairs, optimizing the objective function to maximize Semblance energy and achieve the best NMO correction for the first synthetic data. The optimization parameters were set as follows: $\delta t_0 = 0.5$ and $\delta V_{NMO} = 100$ for convergence constraint; seeking 3 pairs in the Semblance panel; a heuristic search range for times ($lb_t$: 0.25, $ub_t$: 2); and bounds for subsurface velocities ($lb_v$: 1,000, $ub_v$: 3,000). Fig. 2(a) illustrates the




(a) (b)

Figure 2: First (a) and second (b) synthetic data sets without NMO correction.

synthetic seismogram on the left, depicting a seismic reflection event with three geological layers. The Semblance panel on the right displays corresponding time-velocity pairs and coherence val-

**DOI:** 10.59254/sbpo-2024-193821
https://proceedings.science/p/193821?lang=pt-br

ues. The optimization algorithm successfully targeted three regions of high coherence, obtaining a reasonable NMO correction.

### 7.2. Second Synthetic Data

Moving on to the second synthetic data, `syn_cmp_mult.su`, which consisted of 49 seismic traces indicating multiple seismic events. The Semblance parameters used were the same as for the first synthetic data, representing a reasonable range for both seismic events.

The parameters for both algorithms in the search were $\delta t_0 = 0.2$ and $\delta V_{NMO} = 300$ for convergence constraint, seeking 2 pairs, and bounds for times ($lb_t$: 0.5, $ub_t$: 3.5) and velocities ($lb_v$: 1,000, $ub_v$: 3,000). Fig. 2(b) shows the synthetic seismogram on the left, displaying multiple reflections of the same event. The Semblance panel on the right indicates reflections associated with the same seismic event and another event located to the right.

## 8. Results and Discussions

To assess solution quality and algorithm equivalence, Wilcoxon hypothesis tests [McKnight and Najab, 2010] were conducted at a 5% significance level ($\alpha$).

In the initial criterion, we examined the equivalence of mean solutions. The null hypothesis ($H_0$) posits that "There is no difference between the mean solutions obtained by *HGWO* and *SA*". With a test value of $p = 0.9698$, we fail to reject $H_0$. This finding is supported by Figs. 3 and 4.

Fig. 3 displays the seismogram with NMO correction on the left and the associated Semblance panel on the right. The hyperbolas are leveled horizontally without overcorrection. The optimization algorithm yielded reasonable time-velocity pairs: (0.5054, 1,990), (1.2265, 2,308), and (1.73, 2,470). Fig. 4 illustrates the seismogram with NMO correction on the left and the asso-

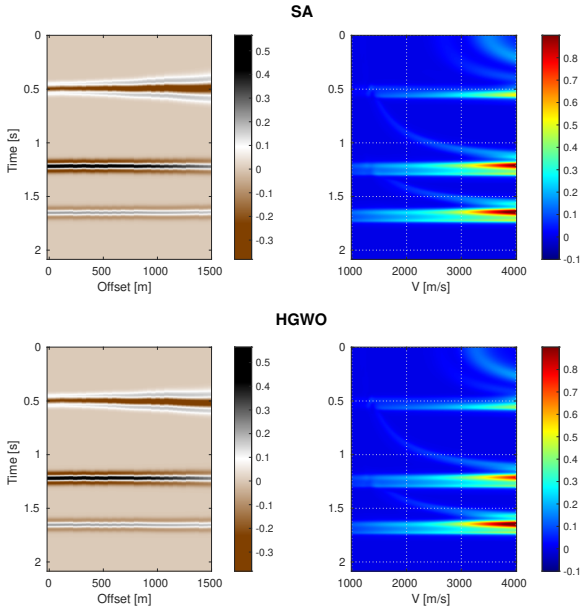



Figure 3: First synthetic data set with NMO correction.

ciated Semblance panel on the right. The optimization algorithm successfully identified solutions that eliminated multiples and maximized Semblance energy. The obtained values for the solution were pairs (1, 1,499) and (2.1, 2,918), aligning well with the expected values for NMO correction.

**DOI:** 10.59254/sbpo-2024-193821
https://proceedings.science/p/193821?lang=pt-br

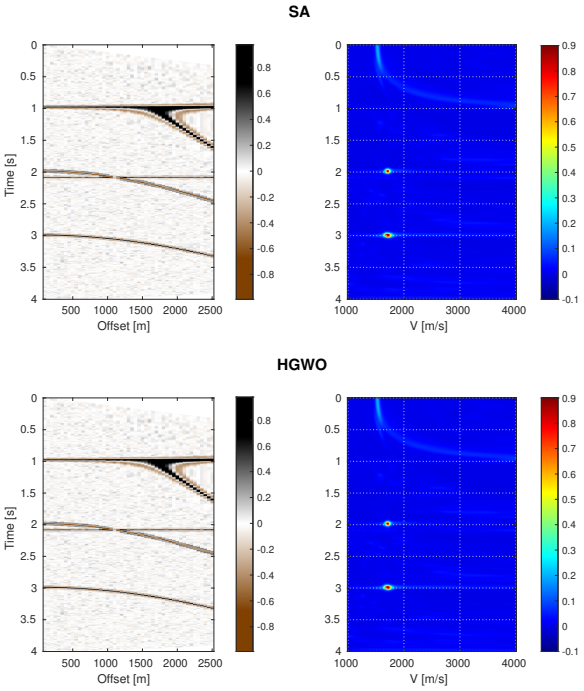



Figure 4: Second synthetic data set with NMO correction.

For the second criterion, we evaluated the equivalence of the objective function costs for obtaining average solutions. The null hypothesis ($H_0$) posits "There is no difference between the costs of average solutions obtained by *HGWO* and *SA*". The test yielded a $p$-value of $0.6666$, indicating that we do not reject the null hypothesis $H_0$.

Finally, we assessed how quickly the objective function is minimized through the total cost. The null hypothesis ($H_0$) states "There is no difference between the sum of costs of solutions obtained by *HGWO* and *SA*". The test yielded a $p$-value of $0.3333$, not rejecting the null hypothesis ($H_0$).

This demonstrates the effectiveness of the *Hybrid Grey Wolf Optimizer* (*HGWO*) and *Simulated Annealing* (*SA*) in obtaining time-velocity pairs for NMO correction, effectively horizontalizing the hyperboles in seismic data. The results obtained showcase the algorithms' ability to fine-tune parameters, resulting in improved coherence and accurate NMO correction, thereby further enhancing the reliability of seismic data processing.

## 9. Conclusion

In summary, this study delved into reflection seismic, a crucial geophysical method for acquiring data in seismic processing, with diverse applications focused on extracting subsurface geological characteristics. The primary objective was to employ automatic techniques for selecting time-velocity pairs, aiming for a reliable NMO correction using the *Hybrid Grey Wolf Optimizer*. A comparative analysis with *Simulated Annealing* was conducted through the Wilcoxon hypothesis test, providing an optimal framework for visualizing geological features after a stacking operation.

The selected techniques, namely the *Hybrid Grey Wolf Optimizer* (*HGWO*) and *Simulated Annealing* (*SA*), were chosen based on the groundwork laid by Velis [2021]. Rigorous experiments were executed on two synthetic datasets, yielding satisfactory results that underscored the efficacy

**DOI:** 10.59254/sbpo-2024-193821
https://proceedings.science/p/193821?lang=pt-br

of both algorithms in solving the automatic selection problem within semblance panels. Notably, statistical analysis revealed no significant difference between the *Hybrid Grey Wolf Optimizer* and *Simulated Annealing*, affirming their comparable performance.

In conclusion, both the *HGWO* and *SA*, as demonstrated in this study and corroborated by Velis [2021], emerged as acceptable methodologies for addressing the automatic selection of time-velocity pairs for NMO correction. This research contributes to the growing body of knowledge supporting the application of these algorithms in seismic data processing, offering valuable insights for future endeavors in this field. Future work will focus on analyzing the performance of these algorithms on real seismic data over large databases.

**Acknowledgements**

This study was financed in part by the Coordenação de Aperfeiçoamento de Pessoal de Nível Superior - Brasil (CAPES) - Finance Code 001.

**References**

Alsadi, H. N. et al. (2017). Seismic hydrocarbon exploration. *2D and 3D Techniques, Seismic Waves. Springer*.

Fortini, C., Maggi, D., Lipari, V., and Ferla, M. (2013). Particle swarm optimization for seismic velocity analysis. In *SEG Technical Program Expanded Abstracts 2013*, p. 4864–4868. Society of Exploration Geophysicists.

Goldberg, D. E. and Richardson, J. (1987). Genetic algorithms with sharing for multimodal function optimization. In *Proc. of the Second International Conference on Genetic Algorithms*, p. 41–49. Hillsdale, NJ: Lawrence Erlbaum.

Granville, V., Krivánek, M., and Rasson, J.-P. (1994). Simulated annealing: A proof of convergence. *IEEE Transactions on Pattern Analysis and Machine Intelligence*, 16(6):652–656.

Hein, N. (1994). Otimização global determinística: Um algoritmo. Master's thesis, Federal University of Santa Catarina.

Holland, J. H. (1992). *Adaptation in Natural and Artificial Systems*. The MIT Press.

Horst, R. and Pardalos, P. M. (2013). *Handbook of Global Optimization*, volume 2. Springer Science & Business Media.

Horst, R., Pardalos, P. M., and Van Thoai, N. (2000). *Introduction to Global Optimization*. Springer Science & Business Media.

Huang, K.-Y., Chen, K.-J., and Yang, J.-R. (2013). Genetic algorithm for seismic velocity picking. In *The 2013 IJCNN*, p. 1–8. IEEE.

Kearey, P., Brooks, M., and Hill, I. (2002). *An Introduction to Geophysical Exploration*, volume 4. John Wiley & Sons.

Kirkpatrick, S., Gelatt Jr, C. D., and Vecchi, M. P. (1983). Optimization by simulated annealing. *Science*, 220(4598):671–680.

Larner, K., Hale, D., Zinkham, S. M., and Hewlett, C. (1982). Desired seismic characteristics of an air gun source. *Geophysics*, 47(9):1273–1284.

**DOI:** 10.59254/sbpo-2024-193821
https://proceedings.science/p/193821?lang=pt-br

Li, S.-Y., Wang, S.-M., Wang, P.-F., Su, X.-L., Zhang, X.-S., and Dong, Z.-H. (2018). An improved Grey Wolf optimizer algorithm for the inversion of geoelectrical data. *Acta Geophysica*, 66: 607–621.

MathWorks, I. (2018). *MATLAB: The Language of Technical Computing. Desktop Tools and Development Environment, Version R2018b*, volume 9. MathWorks.

McKnight, P. E. and Najab, J. (2010). Mann-Whitney U test. *The Corsini Encyclopedia of Psychology*, p. 1–1.

Michalewicz, Z. (1992). *Genetic Algorithms + Data Structures = Evolution Programs*, chapter Evolution Strategies and Other Methods, p. 127–138. Springer Berlin Heidelberg. ISBN 978-3-662-02830-8.

Milkereit, B., Eaton, D., Wu, J., Perron, G., Salisbury, M. H., Berrer, E., and Morrison, G. (1996). Seismic imaging of massive sulfide deposits; Part II, Reflection seismic profiling. *Economic Geology*, 91(5):829–834.

Mirjalili, S., Mirjalili, S. M., Lewis, A., and Optimizer, G. W. (2014). Advances in engineering software. *Renewable and Sustainable Energy Reviews*, p. 46–61.

Mondol, N. H. (2010). Seismic exploration. *Petroleum Geoscience*, 1:375–402.

Payton, C. E. (1977). *Seismic stratigraphy - Applications to hydrocarbon exploration*. American Association of Petroleum Geologists.

Saremi, S., Mirjalili, S. Z., and Mirjalili, S. M. (2015). Evolutionary population dynamics and grey wolf optimizer. *Neural Computing and Applications*, 26(5):1257–1263.

Sen, M. K. and Stoffa, P. L. (2013). *Global Optimization Methods in Geophysical Inversion*. Cambridge University Press.

Sheriff, R. E. and Geldart, L. P. (1995). *Exploration Seismology*. Cambridge University Press.

Song, X., Tang, L., Zhao, S., Zhang, X., Li, L., Huang, J., and Cai, W. (2015). Grey Wolf optimizer for parameter estimation in surface waves. *Soil Dynamics and Earthquake Engineering*, 75: 147–157.

Telford, W., Geldart, L., and Sheriff, R. (1990). *Applied Geophysics*. Cambridge University Press Cambridge.

Törn, A. and Žilinskas, A. (1989). *Global Optimization*, volume 350. Springer.

Vandekerckhove, J. (2008). General simulated annealing algorithm (http://www. mathworks. com/matlabcentral/fileexchange/10548), MATLAB central file exchange.

Vashisth, D., Shekar, B., and Srivastava, S. (2022). Joint inversion of rayleigh wave fundamental and higher order mode phase velocity dispersion curves using multi-objective Grey Wolf optimization. *Geophysical Prospecting*, 70(3):479–501.

Velis, D. (2021). Simulated annealing velocity analysis: Automating the picking process. *Geophysics*, 86(2):V119–V130.

Yilmaz, Ö. (2001). *Seismic Data Analysis: Processing, Inversion, and Interpretation of Seismic Data*. Society of Exploration Geophysicists.

**DOI:** 10.59254/sbpo-2024-193821
https://proceedings.science/p/193821?lang=pt-br